

# We are IntechOpen, the world's leading publisher of Open Access books Built by scientists, for scientists

## 4,800

Open access books available

## 122,000

International authors and editors

## 135M

Downloads

Our authors are among the

## 154

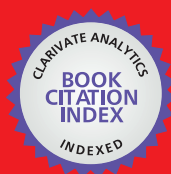
Countries delivered to

## TOP 1%

most cited scientists

## 12.2%

Contributors from top 500 universities

**WEB OF SCIENCE™**

Selection of our books indexed in the Book Citation Index  
in Web of Science™ Core Collection (BKCI)

Interested in publishing with us?  
Contact [book.department@intechopen.com](mailto:book.department@intechopen.com)

Numbers displayed above are based on latest data collected.  
For more information visit [www.intechopen.com](http://www.intechopen.com)



# Electronic Nose System and Artificial Intelligent Techniques for Gases Identification

Iman Morsi

*Arab Academy for Science and Technology,  
Electronics and Communications Department  
Alexandria-Egypt*

## 1. Introduction

Electronic nose is the intelligent design to identify food flavors, cosmetics and different gas odors, depending on sensors. The continuous developing of these sensors permit advanced control of air quality, as well as, high sensitivity to chemical odors. Accordingly, a group of scientists have worked on developing the properties of sensors, while others have modified ways of manufacturing ultra low-cost design (Josphine & Subramanian , 2008); (Wilson et al., 2001).

In the design of an electronic nose, sampling, filtering and sensors module, signal transducers, data preprocessing, feature extraction and feature classification are applied. (Getino et al., 1995) is used as an integrated sensor array for gas analysis in combustion atmosphere in the presence of humidity and variation in temperature from 150-350°C. The sensor array exposed to a gas mixture formed by N<sub>2</sub>, O<sub>2</sub>, CO<sub>2</sub>, H<sub>2</sub>S , HCL and water vapour with a constant flow rate of 500 ml/ min was studied. (Marco et al., 1998). The gas identification with tin oxide sensor array is investigated, in addition, the several undesirable characteristics such as slow response, non-linearties, long term drifts are studied. Correction of the sensor's drift with adaptive self organizing maps permit success in gas classification problems.(Wilson et al., 2001) is introduced as a review of three commonly used gas sensors which are, solid state gas sensor, chemical sensors and optical sensors. Comparisons are deducted among them in terms of their ability to operate at low power, small size and relatively low cost with numerous interference and variable ambient conditions.(Dong Lee & Sik Lee, 2001) depended on solid state gas sensor, thus the pollutants of environment are controlled relative to the sensing mechanism, the sensing properties of solid - state gas sensors to environmental gases, such as No, Co and volatile organic compounds.(Guardado et al. , 2001) is used as a neural network efficiency for the detection of incipient fault in power transformers. The NN was trained according to five diagnosis criteria and then tested by using a new set of data.

This study shows that NN rate of successful diagnosis is dependent on specific criterion under consideration with values in the range of 87-100 %.( Zylka & Mazurek, 2002) introduced a rapid analysis of gases by means of a portable analyzer fitted with

electrochemical gas sensor. The analyzer, which was built, is controlled by a microprocessor and the system incorporates only two gases which are Co and H<sub>2</sub>.

The drawback is the lack of sensors selectivity which is disadvantageous in most applications. (Belhovari et al., 2004; Belhovari et al., 2005) used sensors array with gas identification and Gaussian mixture models. Some problems are studied such as drift problem and slow response is introduced. Robust detection is applied through a drift counteraction approach which is based on extending the training data set using a simulated drift. (Belhovari et al., 2006) gas identification is introduced using sensors array, and different neural networks algorithms. Different classifiers are used MLP, RBF, KNN, GMM and PPCA are compared with each other using the same gas data set allowed performance up to 97%. Electronic gas sensors based on tin oxide films are used for the identification of gases, detection of toxic contaminants and separation of mixture of gases (Kolen, 1994); (Belhovari et al., 2005); (Marco et al., 1998); (Getino et al., 1995); (Becker et al., 2000); (Amigoni et al., 2006).

The problem here is to identify or to discriminate different gases such as, methane, propane, butane, carbon dioxide and hydrogen. Using different concentrations. Taguchi gas sensors (TGS) are used, which is a metal oxide semiconductor sensor, based on tin oxide that has been commercially available from Figaro engineering company (Figaro sensor.com "on - line"). In the design of electronic nose systems, power consumption directly related to temperature operation, selectivity, sensitivity, and stability typically has the most influence on the choice of metal oxide films for a particular application (Fleming, 2001); (Carullo, 2006). For electronic nose applications (Morsi-b, 2008); (Luo et al, 2002); (Bourgeois et al., 2003); (Carullo, 2006) metal oxide semiconductors are largely hampered by their power consumption demands. Thermal isolation and intermittent operation of the heaters reduce the power consumption of the sensors themselves to facilitate their use of importable applications. However, it also presents significant obstacles in terms of noise, drift, aging, and sensitivity to environmental parameters. The Feed Forward Back Propagation of Neural Network using the multilayer perceptron is used to separate between them. Fuzzy logic is used to discriminate different gases and to detect the concentration of each gas. Electronic nose design provides rapid responses, ease of operation and sufficient detection limits. Data quality objectives (DQOs) of gases must be considered as a part of technology development and a focus should be made on the most urgent problems.

### Organization of the chapter

1. Introduction.
2. Experimental setup.
3. Results and analysis.
4. Surface response modeling algorithms and analysis of variance (ANOVA).
5. Separation of butane and propane as a gas mixture using an artificial intelligent technique of Neural Networks.
6. On-line identification of gases using artificial intelligent techniques of Fuzzy Logic.
7. Conclusion.
8. Acknowledgement.
9. References.

## 2. Experimental Setup

The analysis and the characterization of gases are acquired by building a prototype of multi-sensors monitoring system (electronic nose), which are TGS 822, TGS 3870, TGS 4160 and TGS 2600, from Figaro sensor industry, temperature sensor, humidity sensor and supply voltage equal to 5 V. However, current monitoring methods are costly and time intensive, likewise limitations and analytical techniques exist. Clearly, a need exists for accurate, inexpensive, long-term monitoring using sensors. TGS 822 is tin dioxide ( $\text{SnO}_2$ ) as semiconductor. The sensor's conductivity increases, depending on the gas concentration. It has high sensitivity to the vapors of organic solvents, as well as, combustible gases. TGS 2600 is comprised of metal oxide semiconductor layer formed on an alumina substrate of a sensing chip together with an integrated heater. TGS 3870 is a metal oxide semiconductor gas sensor, embedding a micro-bead gas sensing structure. TGS 4160 is a hybrid sensor unit composed of a carbon dioxide sensitive element and a thermistor. All presented sensors have features of long life, low cost, small size, simple electrical circuit, low power consumption and are available in commercial application. The experimental equipment consists basically of the gas bottle mass flow controllers, sensor chamber with volume 475  $\text{cm}^3$ , supply voltage of 5 V and a heating system (Morsi, 2007); (Morsi-a, 2008). Gases used in the experiment are carbon dioxide, hydrogen, methane, propane, butane and a mixture of propane and butane. All measurements are presented at 45% relative humidity. All sensors are connected as an array and covered by a chamber, which has "in" and "outlet" ports. The input is connected with the mass flow controllers to control the concentration of input gas after purging with humidified air. All sensors are subjected to variation in temperatures from ambient temperatures and up (Clifford et al., 2005); (Fleming, 2001). Four variable resistances are connected in series to the four sensors, placed out of chamber, then are followed by the microcontroller, to control and monitor the output of each sensor (Smulko, 2006). The output of the microcontroller is monitored and recorded every 20 sec. Different gases concentrations are applied 100 ppm, 400 ppm, 700 ppm, 1000 ppm with different environmental temperatures between 20°C to 50°C with different variable resistances for each sensor  $R_L = 1 \text{ k}\Omega$ , 3  $\text{k}\Omega$ , 5  $\text{k}\Omega$ , and 7  $\text{k}\Omega$ . Variable load resistance is used to control the conductivity and to increase the selectivity of each gas than other gases. Sensitivity is used to refer either to the lowest level of chemical concentration that can be detected or to the smallest increment of concentration that can be detected in the sensing environment. While selectivity refers to the ratio of the sensor's ability to detect what is of interest over the sensor's ability to detect what is not of interest as the interferences. Sensors for use in electronic nose need partial selectivity, mimicking the responses of the olfactory receptors in the biological nose (Belhovari et al., 2006). Figure (1) shows the electronic nose gas system. The hardware requirements for the system implementation include a microcontroller Pic 16 F 877A with embedded (A/D) converter. It is chosen for the implementation of this task due to the on chip memory resources, as well as, its high speed. The output data is transferred to a PC via a serial port RS 232 with a Baud rate of 2400 from the microcontroller. The software is developed in C language and is compiled, assembled, and downloaded to the system. The output volt of each sensor is collected, stored in memory and transferred to a microcontroller to be ready for the processing work and the temperature is also monitored via a temperature sensor and is recorded (Ishida et al., 2005); (Weigong et al., 2006); (Smulko, 2006).



Fig. 1-a. Electronic nose of gas detection with chamber



Fig. 1-b. Electronic nose of gas detection without chamber

Measurements using the electronic nose gas system detector have been done according to three parts: measurement part, mathematical analysis part, and presentation part. The system is supported by a collection of methods to improve the uncertainty and reliability. Different processing techniques like self calibration, self validation and statistical analysis methods are included. Data averaging standard deviation calculation are used to test and evaluate the performance of the whole measuring system in order to minimize error (Morsi, 2007); (Morsi – a, 2008).

### 3. Results and Analysis:

The design of electronic nose depends on physical connectivity of the sensors, relating to the data management, computing management and knowledge discovery management, which are associated with the sensors and the data they generate, and how they can be addressed within an open computing environment. Eventually, the issue relates to the integrated analysis of the sensor data depending on the variation of gases respectively. Moreover, there is a correlation and interaction of data.

Hence, the use of standardized data access and integration techniques to assess and integrate such data is essential. Furthermore, if the analysis is to proceed over large data sets, it is essential to provide high performance computing resources to allow rapid computation to proceed. Measurements have been done using the described experimental setup. The gas is injected inside the chamber and the concentration in ppm is controlled through the mass flow controller. Extensive measurements are performed and data collected from gas sensor via microcontroller undergoes a processing stage. Due to variation in temperature from 20°C to 50°C, the load resistance is adjusted to 1 k $\Omega$ , 3 k $\Omega$ , 5 k $\Omega$  and 7 k $\Omega$ , respectively and the gas concentrations are adjusted to 100 ppm, 400 ppm, 700 ppm and 1000 ppm respectively. There is an output voltage of each sensor relative to the variation of these parameters. The extensive numbers of measured values have been extracted at each resistance with different concentrations. The measurement values of different parameters with different gases at  $R_L = 7 \text{ k}\Omega$  are described by figs 2 till 13 as a specimen deducted from enormous measured data due to different variable resistances with different concentrations (Morsi –a , 2008) .



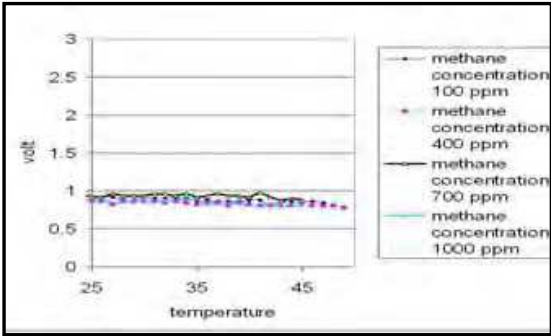


Fig. 2. Methane gas with TGS 3870 at  $R_L$  7 k $\Omega$

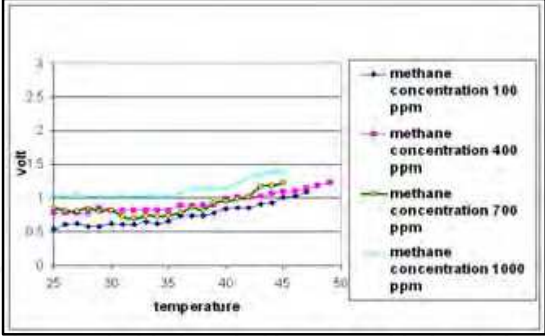


Fig. 3. Methane gas with TGS 822 at  $R_L$  7 k $\Omega$

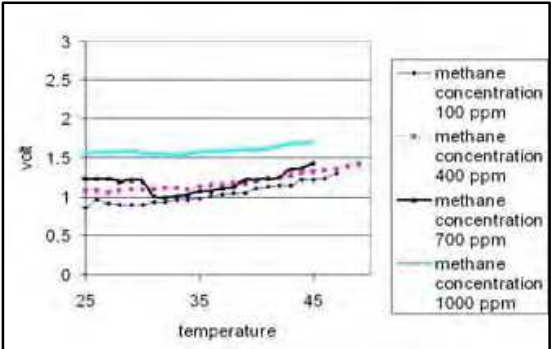


Fig. 4. Methane gas with TGS 2600 at  $R_L$  7 k $\Omega$

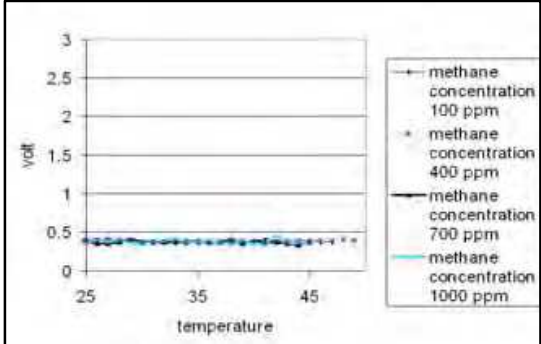


Fig. 5. Methane gas with TGS 4160 at  $R_L$  7 k $\Omega$

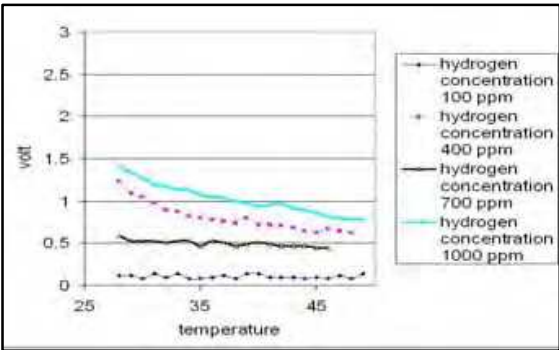


Fig. 6. Hydrogen gas with TGS 3870 at  $R_L$  7 k $\Omega$

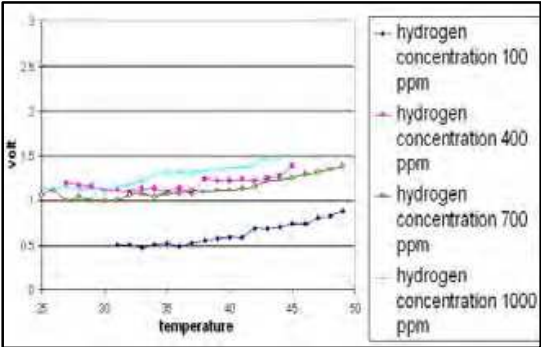


Fig. 7. Hydrogen gas with TGS 822 at  $R_L$  7 k $\Omega$

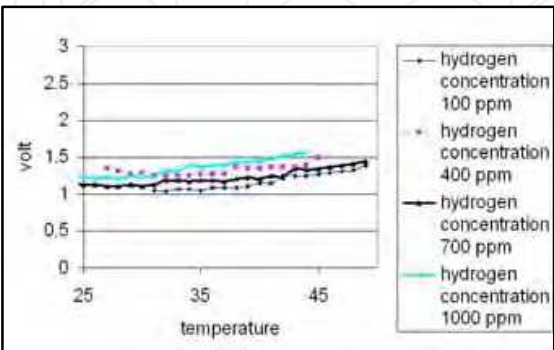


Fig. 8. Hydrogen gas with TGS 2600 at  $R_L$  7k $\Omega$

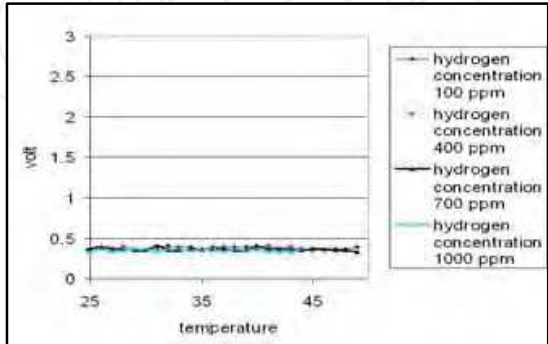


Fig. 9. Hydrogen gas with TGS 4160 at  $R_L$  7 k $\Omega$

Figures 14, 15 and 16 show resistances fluctuations with different sensors, different gases and constant concentration at 700 ppm (Morsi – a, 2008).

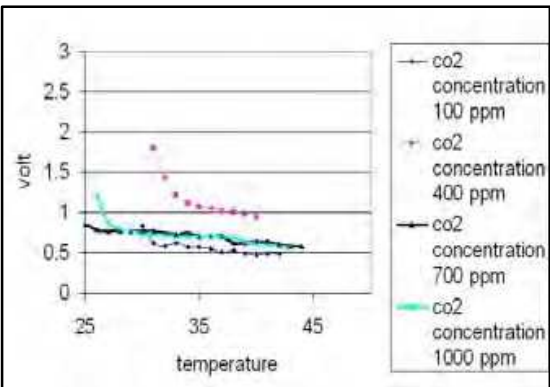


Fig. 10. Carbon dioxide gas with TGS 3870 at  $R_L$  7 k $\Omega$

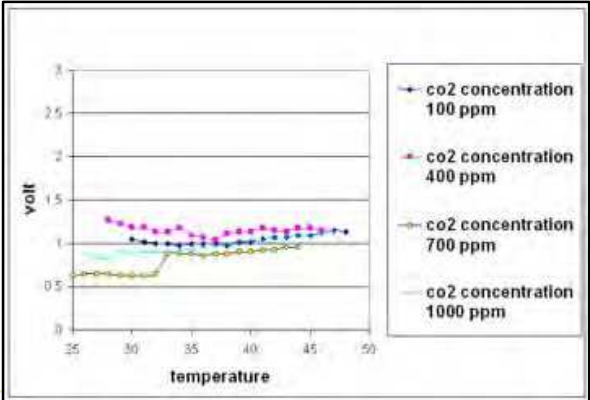


Fig. 11. Carbon dioxide gas with TGS 822 at  $R_L$  7 k $\Omega$

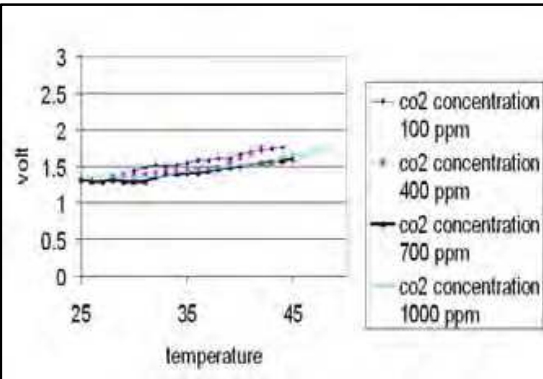


Fig. 12. Carbon dioxide gas with TGS 2600 at  $R_L$  7 k $\Omega$

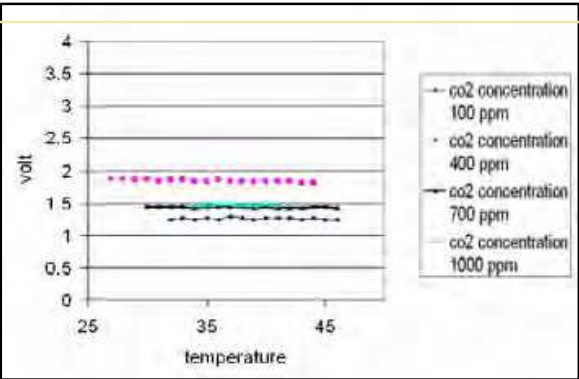


Fig. 13. Carbon dioxide gas with TGS 4160 at  $R_L$  7 k $\Omega$

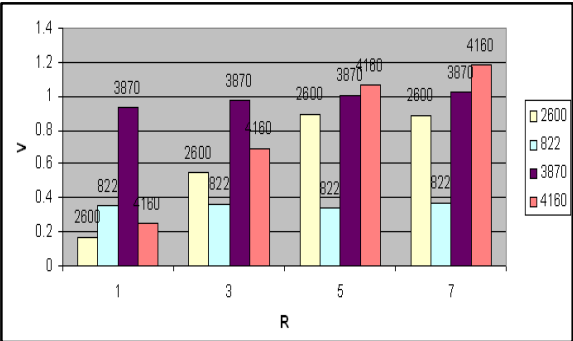


Fig. 14. Methane gas at concentration 700 ppm

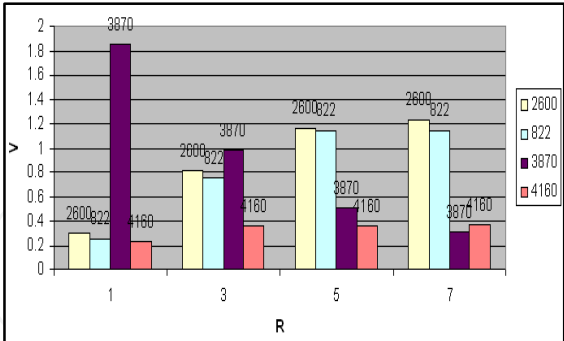


Fig. 15. Hydrogen gas at Concentration 700 ppm

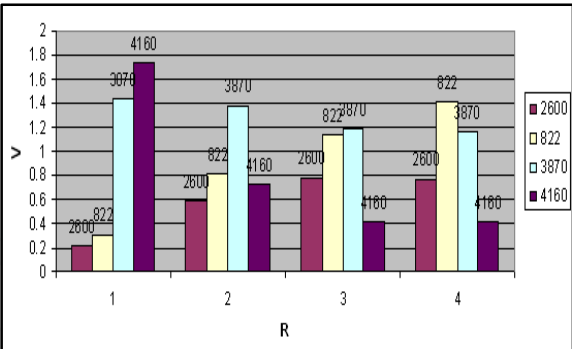


Fig. 16. Carbon dioxide gas at concentration 700 ppm

The Electronic nose system used for gas detection depends on the resistance variation of the gas sensor, which given the possibility increases the selectivity and sensibility. The portable and cheap electronic nose is based on commercially available gas sensors. The stability of the sensors, as well as, their sensitivity depends on the ratio between the change in sensor resistance in the presence or absence of the gas, which was experimentally characterized. Moreover, the method can reduce the number of gas sensors to limit power consumption and maintenance costs. From figs 14 , 15 and 16 it can be noticed that, by increasing load resistance from 1 k $\Omega$  to 7 k $\Omega$ , the output volt of TGS 822, TGS 2600 is directly proportional (i.e. increase with load resistance), However, TGS 3870 is inversely proportional by increasing load resistance incase of hydrogen and carbon dioxide. TGS 4160 remains constant with average output volt in the range (0.2-0.4) V incase of hydrogen, but incase of carbon dioxide TGS 4160 gives variation in the output voltage from (0.4 - 1.8) V. This variation is inversely proportional to the load resistance variation, which concludes that this sensor is preferable to detect carbon dioxide than other gases.

It can also illustrate the sensitivity of each sensor due to the resistance fluctuation. The output results include non-linear response, drift and slow response time. The main problem is the drift, which causes significant temporal variations of the sensor response when exposed to the same gas under identical conditions (Clifford et al., 2005); (Fleming, 2001). It is noticed that response times depend on many parameters, such as the material type, operating temperature, thickness of the semiconductor, variable resistance, humidity as well as gas concentration. The sensor array reacts slowly and takes an average of 10 min to reach the stationary state. This time is a combination of the time to fill the chamber and the sensor response time. To achieve robust and fast identification of combustion gases with an array of sensors, a recent study suggested three main methods for reducing response time:

1. Increasing operating temperature.
2. Reducing the film thickness.
3. Using variable resistance to reduce the number of sensors and the power consumption of the system.



4. Surface Response Modeling Algorithms and Analysis of Variance (ANOVA)

In the system design, surface response models investigated are very useful in understanding the functional relationships between a set of independent factors.

The relationship can be expressed as a mathematical equation which describes the response of the independent factors and a set of parameters. The surface response models depend on observing input and output values of the actual and predicted parameters, which is known by the system model identification (SMI). The resulting empirical models of SMI can be used to: (1) Predict the system behaviour over a specified designed space, (2) Illustrate the mathematical relationships and interactions between input and output of the system (3) Optimize the system performance (4) Select the appropriate factor values that satisfy system performance goals to investigate the performance prediction accuracy of different algorithms, thus the predicted results generated by each empirical model is compared with actual measured results to provide a comparison and identify the advantages of each algorithm.

In the present work, different empirical models are used to detect the response of the surface of each gas. By entering the voltage of each sensor, load resistance and temperature as an input thus predicts the concentration as an output. The following are the used four empirical models:

Linear

Y = b<sub>0</sub> + b<sub>1</sub> x<sub>1</sub> + b<sub>2</sub> x<sub>2</sub> + b<sub>3</sub> x<sub>3</sub>. (1)

Interaction

Y= b<sub>0</sub> + b<sub>1</sub> x<sub>1</sub>+ b<sub>2</sub> x<sub>2</sub>+ b<sub>3</sub> x<sub>3</sub>+ b<sub>12</sub> x<sub>1</sub> x<sub>2</sub>+ b<sub>13</sub> x<sub>1</sub> x<sub>3</sub>+ b<sub>23</sub> x<sub>2</sub> x<sub>3</sub>. (2)

Pure Quadratic

Y= b<sub>0</sub> + b<sub>1</sub> x<sub>1</sub> + b<sub>2</sub> x<sub>2</sub> + b<sub>3</sub> x<sub>3</sub> + b<sub>11</sub> x<sub>12</sub> + b<sub>22</sub> x<sub>22</sub> + b<sub>33</sub> x<sub>33</sub>. (3)

Full Quadratic

Y = b<sub>0</sub> + b<sub>1</sub> x<sub>1</sub> + b<sub>2</sub> x<sub>2</sub> + b<sub>3</sub> x<sub>3</sub> + b<sub>12</sub> x<sub>1</sub> x<sub>2</sub> + b<sub>13</sub> x<sub>1</sub> x<sub>3</sub> + b<sub>23</sub> x<sub>2</sub> x<sub>3</sub> + b<sub>11</sub> x<sub>12</sub> + b<sub>22</sub> x<sub>22</sub> + b<sub>33</sub> x<sub>23</sub>. (4)

Where

Y is the predicting concentration of each gas.  
x<sub>1</sub>, x<sub>2</sub>, x<sub>3</sub> are voltages of each sensor, load resistance, and temperature, respectively.  
B<sub>ij</sub> is the effect of element i on element j or the effect of first input on the second input, i and j have values from 1 to 3.  
More than 300 readings for each input are used to detect the error. The concentrations of each gas are stored in matrices, which are related to the output voltage of each sensor through a regression coefficient matrix and the equations can be solved using surface response empirical models to predict the concentrations. Then, the percentage error can be calculated between actual concentration and predicted concentration to determine the best empirical modeling algorithm, which describes the surface response of each gas and has the least error. Table1 shows the percentage error for the different gases with different surface response empirical modeling algorithms (Morsi – a, 2008).

<div>Empirical Modeling Algorithms</div> <div><i>Gases</i></div>	The Percentage Error of Carbon Dioxide	The Percentage Error of Hydrogen	The Percentage Error of Methane
Sensor Type	TGS 822		
Linear	21.322%	13.745%	20.048%
Interactions	19.613%	0.2439%	21.175%
Pure Quadratic	17.7612%	11.2664%	17.9546%
Full Quadratic	14.2644%	0.096.029%	14.426%
Sensor Type	TGS 2600		
Linear	18%	9.2%	2.2%
Interactions	11%	7.7%	5.5%
Pure Quadratic	30.5%	12.95%	5.8%
Full Quadratic	8%	5.5%	5.7%
Sensor Type	TGS 3870		
Linear	6.41%	1.66%	3.47%
Interactions	3.03%	1.1%	0.98%
Pure Quadratic	2.08%	2.3%	0.28%
Full Quadratic	1.68%	0.641%	0.02%
Sensor Type	TGS 4160		
Linear	6.6534%	49.925%	51.572%
Interactions	8.1904%	53.159%	51.253%
Pure Quadratic	8.9625%	45.646%	44.386%
Full Quadratic	7.0078%	40.353%	44.358%

Table 1. Comparisons of different empirical modeling algorithms with different sensors and different gases.

It can be noticed that, for the three different gases, four different algorithms are used. Thus, full quadratic algorithms can predict the concentration of each gas with less error than other algorithms. From the percentage error, it is clear that in the case of TGS 822, TGS 2600 and TGS 3870 gas sensors provide the least error in the case of methane than hydrogen. It is preferred to use this sensor to detect hydrogen and methane. However, it is unpreferable in the case of carbon dioxide. It is also noticed that in TGS 4160 gas sensor is preferable to be carbon dioxide, where as the highest errors are recorded in the case of hydrogen and methane.

From the above results, it can be concluded that the surface response modeling algorithms provide accurate detection for different concentrations of gases depending on solving regression matrices using different equations while detecting the percentage error between the actual and the predicted measurements. The key challenges for building regression algorithms determine the significant factors that are included in the final mathematical equation and quantify the effects of those factors. Tables 2, 3 and 4 show the ANOVA results for each sensor with different gases. The second column is the degree of freedom (DF). The mean square (MS) is the variance of the data for each factor interaction. The sum of squares (SS) is computed as  $MS \times DF$ . F-statistic is defined as the ratio of MS to Error. P-value is the smallest probability of rejecting the null hypothesis. Using the analysis of variance (ANOVA), it is possible to identify those effects that are statistically significant. It can be noticed that, the variance is not constant and if the output voltage has a high value, the variance also has a high value for different gases. The resulting algorithm includes only those independent factors that are statistically significant ( $P\text{-value} < 0.05$ ). Quantifying the main and two-way interaction effects of the independent factors are equivalent to using the well-known method of least squares fitting method in order to compute the regression coefficients (Morsi-a, 2008) .

Source	Sum Sq.	d.f.	Mean Sq.	F	Prob>F
X1	4.98058	3	1.66019	116.18	0
X2	0.13867	3	0.04622	3.23	0.0257
X3	0.05372	11	0.00488	0.34	0.9738
X1*X2	1.89822	9	0.21091	14.76	0
X1*X3	0.33692	33	0.01021	0.71	0.8624
X2*X3	0.19688	33	0.00597	0.42	0.9972
Error	1.34323	94	0.01429		
Total	9.95126	186			

Table 2-a. Anova of methane gas with TGS 3870 gas sensor

Source	Sum Sq.	d.f.	Mean Sq.	F	Prob>F
X1	2.32996	3	0.77665	511.05	0
X2	0.18818	3	0.06273	41.27	0
X3	0.01857	11	0.00169	1.11	0.3617
X1*X2	0.42355	9	0.04706	30.97	0
X1*X3	0.03739	33	0.00113	0.75	0.8291
X2*X3	0.06018	33	0.00182	1.2	0.2453
Error	0.14285	94	0.00152		
Total	3.40834	186			

Table 2-c. Anova of methane gas with TGS 2600 gas sensor

Source	Sum Sq.	d.f.	Mean Sq.	F	Prob>F
X1	10.0555	3	3.35183	341.8	0
X2	0.6069	3	0.20229	20.63	0
X3	0.166	11	0.01509	1.54	0.1306
X1*X2	1.5482	9	0.17203	17.54	0
X1*X3	0.2412	33	0.00731	0.75	0.8293
X2*X3	0.1651	33	0.005	0.51	0.9847
Error	0.9218	94	0.00981		
Total	15.7931	186			

Table 2-b. Anova of methane gas with TGS 822 gas sensor

Source	Sum Sq.	d.f.	Mean Sq.	F	Prob>F
X1	0.00687	3	0.00229	6.03	0.0008
X2	0.01906	3	0.00635	16.72	0
X3	0.00246	11	0.00022	0.59	0.8346
X1*X2	0.04452	9	0.00495	13.02	0
X1*X3	0.01365	33	0.00041	1.09	0.3658
X2*X3	0.01377	33	0.00042	1.1	0.3545
Error	0.03572	94	0.00038		
Total	0.13722	186			

Table 2-d. Anova of methane gas with TGS 4160 gas sensor

Source	Sum Sq.	d.f.	Mean Sq.	F	Prob>F	Source	Sum Sq.	d.f.	Mean Sq.	F	Prob>F
X1	6.9938	3	2.33128	157.37	0	X1	26.7364	3	8.91215	57.34	0
X2	0.3428	3	0.11428	7.71	0.0001	X2	2.5009	3	0.83363	5.36	0.0019
X3	0.1795	11	0.01631	1.1	0.369	X3	0.6347	11	0.0577	0.37	0.9642
X1*X2	1.2806	9	0.14229	9.6	0	X1*X2	13	9	1.44444	9.29	0
X1*X3	0.3798	33	0.01151	0.78	0.7921	X1*X3	2.8352	33	0.08591	0.55	0.9722
X2*X3	0.6352	33	0.01925	1.3	0.1647	X2*X3	7.7506	33	0.23487	1.51	0.0634
Error	1.3925	94	0.01481			Error	14.6111	94	0.15544		
Total	12.7402	186				Total	66.6705	186			

Table 3-a. Anova of hydrogen gas with TGS 3870 gas sensor

Table 4-a. Anova of carbon dioxide gas with TGS 3870 gas sensor

Source	Sum Sq.	d.f.	Mean Sq.	F	Prob>F	Source	Sum Sq.	d.f.	Mean Sq.	F	Prob>F
X1	14.339	3	4.77966	947.25	0	X1	22.3335	3	7.4445	61.91	0
X2	0.8761	3	0.29205	57.88	0	X2	1.154	3	0.38466	3.2	0.0269
X3	0.019	11	0.00173	0.34	0.9738	X3	0.6538	11	0.05944	0.49	0.9025
X1*X2	2.0629	9	0.22921	45.43	0	X1*X2	12.6893	9	1.40992	11.73	0
X1*X3	0.2706	33	0.0082	1.63	0.0362	X1*X3	1.1833	33	0.03586	0.3	0.9999
X2*X3	0.481	33	0.01457	2.89	0	X2*X3	2.157	33	0.06536	0.54	0.9754
Error	0.4743	94	0.00505			Error	11.3033	94	0.12025		
Total	20.4315	186				Total	55.1715	186			

Table 3-b. Anova of hydrogen gas with TGS 822 gas sensor

Table 4-b. Anova of carbon dioxide gas with TGS 822 gas sensor

Source	Sum Sq.	d.f.	Mean Sq.	F	Prob>F	Source	Sum Sq.	d.f.	Mean Sq.	F	Prob>F
X1	13.7397	3	4.5799	672.08	0	X1	18.6028	3	6.20092	232	0
X2	0.3778	3	0.12592	18.48	0	X2	1.08	3	0.35999	13.47	0
X3	0.074	11	0.00673	0.99	0.4632	X3	0.2586	11	0.02351	0.88	0.5628
X1*X2	2.0214	9	0.2246	32.96	0	X1*X2	7.5837	9	0.84263	31.53	0
X1*X3	0.247	33	0.00748	1.1	0.3541	X1*X3	0.6088	33	0.01845	0.69	0.8857
X2*X3	0.1528	33	0.00463	0.68	0.8954	X2*X3	0.923	33	0.02797	1.05	0.4189
Error	0.6406	94	0.00681			Error	2.5124	94	0.02673		
Total	19.635	186				Total	32.1458	186			

Table 3-c. Anova of hydrogen gas with TGS 2600 gas sensor

Table 4-c. Anova of carbon dioxide gas with TGS 2600 gas sensor

Source	Sum Sq.	d.f.	Mean Sq.	F	Prob>F	Source	Sum Sq.	d.f.	Mean Sq.	F	Prob>F
X1	0.00826	3	0.00275	8.08	0.0001	X1	0.03518	3	0.01173	18.08	0
X2	0.00037	3	0.00012	0.36	0.7818	X2	0.03206	3	0.01069	16.47	0
X3	0.00914	11	0.00083	2.44	0.0101	X3	0.00647	11	0.00059	0.91	0.5377
X1*X2	0.01784	9	0.00198	5.82	0	X1*X2	0.10369	9	0.01152	17.76	0
X1*X3	0.01671	33	0.00051	1.49	0.0714	X1*X3	0.03503	33	0.00106	1.64	0.0342
X2*X3	0.01413	33	0.00043	1.26	0.1966	X2*X3	0.02637	33	0.0008	1.23	0.2165
Error	0.03203	94	0.00034			Error	0.06097	94	0.00065		
Total	0.09954	186				Total	0.32414	186			

Table .3-d. Anova of hydrogen gas with TGS 4160 gas sensor

Table 4-d. Anova of carbon dioxide gas with TGS 4160 gas sensor

## 5. Separation of Butane and Propane as a Gas Mixture Using an Artificial Intelligent Neural Network

The use of natural gas has been increasingly adapted as butane and propane exist in both industry and as a fuel in domestic applications. One of the most important problems in the gas detection field is that there is a strong demand to detect butane and propane as pure gases which are used as fuel; however, both are extracted from the natural gas mixed with each other. The calibration of both gases in the pure case and also as a mixture at different temperatures using electronic nose system is studied. Also, a study is done for the efficiency of feed forward back propagation neural network for the detection of gases using the multilayer perceptron (MLP) methods to differentiate between them depending on the data driven from the electronic nose gas system (Morsi - a, 2008).

Butane ( $C_4H_{10}$ ): a normally gaseous straight-chain or branch-chain hydrocarbon is derived from natural gas or from refinery gas streams. It includes isobutane and normal butane and is used for cooking, heating, as a household fuel, propellant or refrigerant, where, it is commonly used in UK. It is slightly toxic by inhalation, as it causes central nervous system depression at high concentrations, and is used in the manufacture of rubber and fuels (Morsi -a, 2008).

Propane ( $C_3H_8$ ): a normally gaseous straight- chain hydrocarbon is a colorless paraffinic gas that boils at a temperature of  $-42\text{ }^{\circ}\text{C}$ . It is extracted from natural gas or refinery gas streams. Under normal atmospheric pressure and temperature, it exists in a gaseous state. However, propane is usually liquified through pressurization for transportation and storage. It is primarily used for heating or cooking, as a fuel gas in areas not serviced by natural gas, and as a petrochemical fuel stock. Propane is used in forklifts because it offers the best performance in power, speed and saves money on fuel costs. It is also used in agriculture as an alternative to conventional pesticides and herbicides and in outdoor grills (Morsi -a, 2008).

Neural Networks with feed forward back propagation training algorithm is used to detect each gas with different sensors. It is combined with gas sensors to address these issues. After a processing stage, the resulting feature vector is used to solve separation problem in case of a mixture, by identifying an unknown sample as one from a set of previously known gases. Multi Layer Perceptron MLP improves linear discrimination techniques in case of a mixture, depending on the data driven from each sensor (Morsi -a, 2008); (Guardado et al., 2001).

Gases used are butane and propane and their mixtures. They are injected into a gas chamber. The sensor detects sequentially the variation in the propane and butane gas concentration and its resistance is modified accordingly. Figures 17 till 32 depict the output voltage of sensors TGS 822, TGS 3870, TGS 2600 and TGS 4160 as functions of temperature, with load resistances  $R_L = 1\text{ k}\Omega$  and  $R_L = 7\text{ k}\Omega$ . The relations are given for butane and propane at concentrations of 100 ppm, 400 ppm, 700 ppm and 1000 ppm respectively. It can be noticed that the detection of both gases can be carried out by TGS 822, TGS 3870, TGS 2600, but not by TGS 4160. It is clear noticed from figs 17-20, that for the TGS 822 gas sensor, the conductivity and sensitivity increase for both butane and propane by increasing concentration and load resistance. The sensitivity is directly proportional to the load resistance. For TGS 3870 gas sensor, Figs 21-24, it can be noticed that the sensitivity and conductivity are inversely proportional with load resistance.



By increasing load resistance, the sensitivity and conductivity will decrease. The difference between the relationship of sensitivity, conductivity and load resistance between both sensors, allows the discrimination between propane and butane depending on the variation of the resistance. For the TGS 2600 gas sensor, figs 25 till 28, the voltage increases with the increase of concentrations, temperature and load resistance for both gases.

With TGS 4160 gas sensor, figs 29-32, for both butane and propane, there is no change in the output volt in load resistance, therefore, we can not depend on this sensor discrimination. The calibration of pure gases among their semiconductor sensor, predicts the correct sensor that should be used in classification. Figures 33 and 34 depict the mixture of both propane and butane injected inside the chamber. Propane has a concentration of 600 ppm while butane has a concentration of 400 ppm. It can be noticed that the output of both gases is unstable, which leads to difficulties in discrimination. Neural Networks (NN) have been used extensively in applications where pattern recognition is needed. They are adaptive, capable of handling highly non-linear relationships and generalizing solutions for a new set of data. In fact, NN do not need a predefined correspondence function, which means that there is no need for a physical model. A neuron model is the most basic information processing unit in a neural network. Depending on the problem complexity, they are organized in three or more layers: the input layer, the output layer and one or several hidden layers. Each neuron model receives input signals, which are multiplied by synaptic weights. An activation function transforms these signals into an output signal to the next neuron model. The Back Propagation learning algorithm is used due to its ability of pattern recognition. A sigmoid activation function was also used because of two reasons: it is highly non-linear and has been reported to have a good performance when working with the back propagation learning algorithms [45][46]. In order to avoid slow training, it is decided to use only three layers. During the training process, a vector from a training set ( $x_i$ ) representing a gas pattern is presented to the net. The winning neuron (the closet to the pattern with an Euclidean), and its neighbours, the neighborhood area, change their position, becoming closer to the input pattern according to the following learning rule:

$$W_{ji}^{new} = W_{ji}^{old} + \zeta(t) \cdot nb(t,d) \cdot (x_i - x_{ji}^{old}) \quad (5)$$

where  $W_{ji}$  are the weights of the neurons inside, the neighborhood area,  $j$  is the index of the neuron,  $i$  is the index of pattern,  $t$  is the time step,  $\zeta(t)$  is the learning rate,  $nb(t,d)$  is the neighborhood function, and  $d$  is the distance between the neuron and the winner measured over the net. The learning rate and the neighborhood are monotonically decreasing functions along the training (Eberhart et al. 1996); (Wesley, 1997). Both patterns constitute an NN training set. In case NN training is slow or shows little convergence, then both patterns are either poorly correlated or incorrect. This study is performed on pure butane and propane gases, and a mixture of them. The data set is divided in two parts. The first is used to train the net, while the second is used to test it. Training patterns are chosen from different concentrations, different times and different temperatures. A large number of patterns have been selected from the extremes of the concentrated range and from initial parts of the dynamic response to give a larger weight to more early difficult cases. The Neural Network is constructed as a feed forwarded back propagation network that is composed of three layers: input, hidden and output layers. The input layer has three neurons corresponding to the output voltages of each sensor ( $x_1$ ), temperature ( $x_2$ ) and variable resistance ( $x_3$ ).

The hidden layer has five neurons. The hidden layer neurons use a transfer function of tansig which is a hyperbolic tangent sigmoid function used to calculate the layer's output from its net input. One hidden layer with 5 neurons is used which gives the least mean square error (MSE) between the actual and the predicted data. The output layer has one neuron corresponding to the concentration of gas. The predicted performance metric,  $y$ , given by the neural network model is as follows.

$$y = \text{Purelin} \left( \sum_{i=1}^5 w_{2i1}, \text{Tansig} \left( \sum_{j=1}^3 w_{1ji} x_j + \theta_{1j} \right) + \theta_{21} \right) \quad (6)$$

Where:  $x_j$  is the input of node  $j$  in the input layer.

$W_{1ji}$  is the weight between node  $j$  in the input layer to node  $i$  in the hidden layer.  $\theta_{1i}$  is the bias of node  $i$  in the hidden layer.  $W_{2i1}$  is the weight between node  $i$  in the hidden layer to the node in the output layer.  $\theta_{21}$  is the bias of the node in the output layer. The numbers 5 and 4 are the numbers of nodes in the hidden layer and in the input layer, respectively, using a simple linear transformation. All performance data are scaled to provide values between -1 and 1. Scaling is performed for two reasons: to provide commensurate data ranges, so that the regressions are not dominated by any variable that happened to be expressed in large number, and to avoid the asymptotes of the sigmoid function. During the training, the weights of the neural network are iteratively adjusted to minimize the network performance function MSE. The validation set is used to stop training early if the network performance on the validation set fails to improve. Test set is used to provide an independent assessment of the model predictive ability. The percentage error is important; 100% error means a zero prediction accuracy and error close to 0% means an increasing prediction accuracy. For the proposed Neural Network model, the percentage error is found to be 0.662%, 0.031%, 0.162%, 1.5% for sensors TGS 822, TGS 3870, TGS 2600 and TGS 4160, respectively. MLP provides an optimized structure which provides linear discrimination between both gases. Figs 35, 36, 37, and 38 depict the MLP results in separating butane and propane gas by using TGS 822, TGS 3870, TGS 2600 and TGS 4160 sensors respectively. The sign circle indicates butane gas where as the sign plus indicates propane gas. Table 5 depicts the results of classification for different gases among the different semiconductor sensors. From the presented results, TGS 3870, TGS 2600 and TGS 822 gas sensor can discriminate both gases rather than TGS 4160 which does not give different response with different conditions. This conclusion is obtained from the multilayer perception of Neural Network. The Neural Network model does not yield a mathematical equation that can be manipulated. However, its strength lies in its ability to accurately predict system performance over the entire design space and its ability to compensate for the inherent information inadequacy by requiring large and well spread training sets. Neural Network with feed forward back propagation is used to detect the concentration of each gas. MLP is able to separate between the mixtures with linear discrimination. TGS 3870 gives the optimum classification with a percentage error of 0.031%, then, TGS 2600 gas sensor can be classified between them with a percentage error 0.162%, then, TGS 822 gas sensor gives percentage error of classification 0.662%. However, TGS 4160 gas sensor failed to discriminate both gases and gives a percentage error of 40%.

Neural Network with MLP method is very robust against sensor nonlinearities, time effects, and error rate depending on the selection of data, which is acquired by different semiconductor gas sensors (Morsi -a, 2008) .

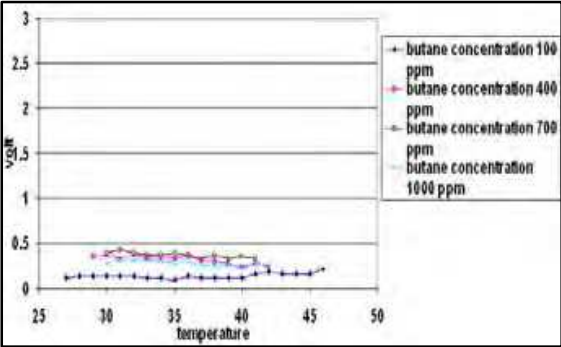


Fig. 17. Butane with TGS 822 at  $R_L$  1  $k\Omega$

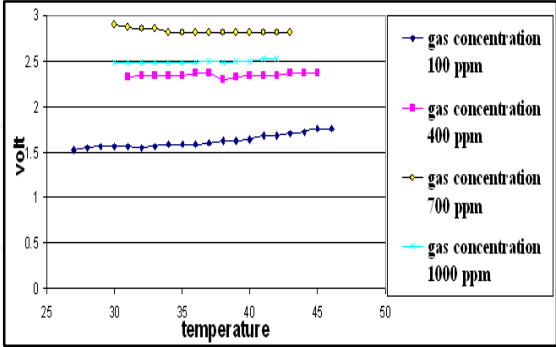


Fig. 18. Butane with TGS 822 at  $R_L$  7  $k\Omega$

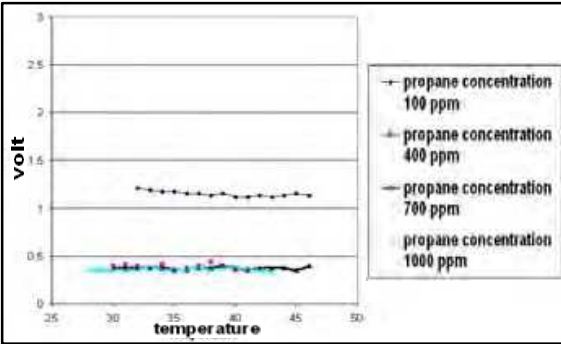


Fig. 19. Propane with TGS 822 at  $R_L$  1  $k\Omega$

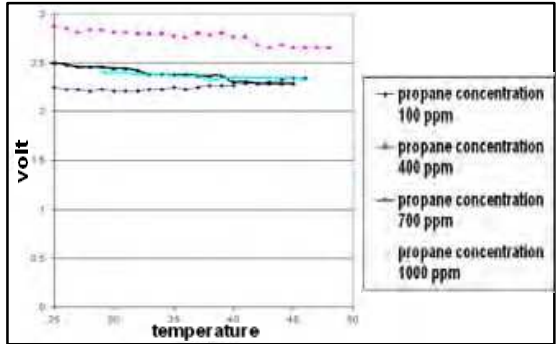


Fig. 20. Propane with TGS 822 at  $R_L$  7  $k\Omega$

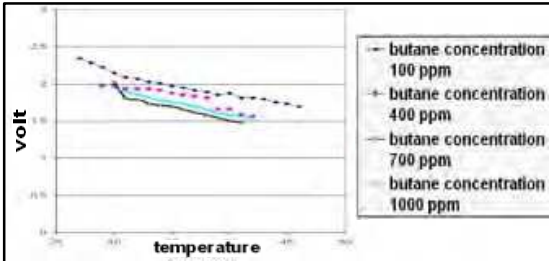


Fig. 21. Butane with TGS 3870 at  $R_L$  1  $k\Omega$

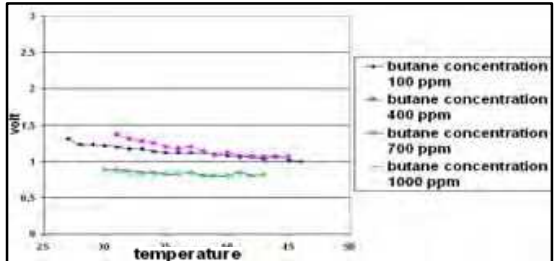


Fig. 22. Butane with TGS 3870 at  $R_L$  7  $k\Omega$

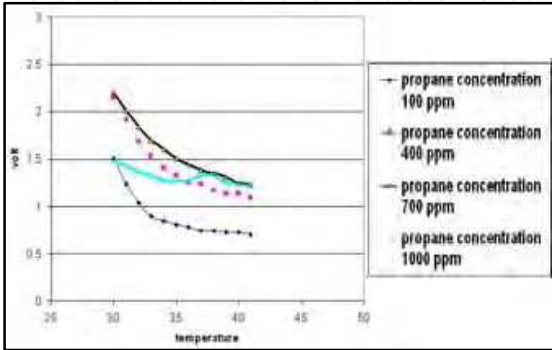


Fig. 23. Propane with TGS 3870 at  $R_L$  1k $\Omega$

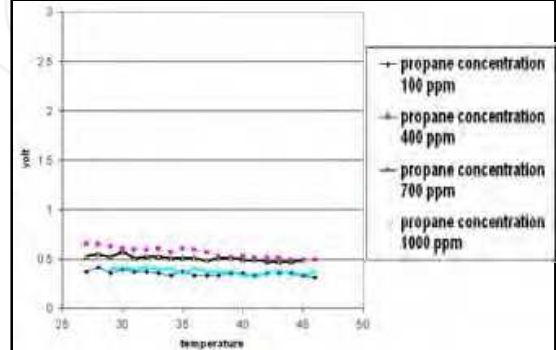


Fig. 24. Propane with TGS 3870 at  $R_L$  7  $k\Omega$

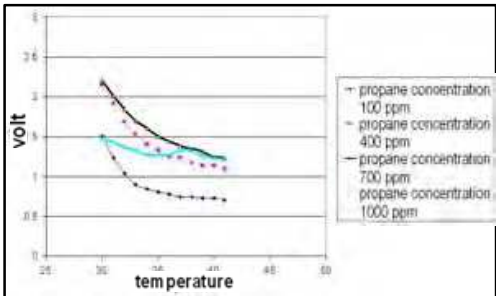


Fig. 23. Propane with TGS 3870 at  $R_L$

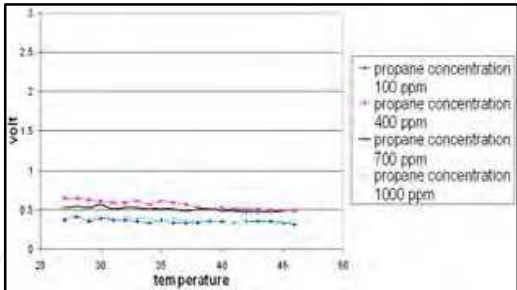


Fig. 24. Propane with TGS 3870 at  $R_L$  7

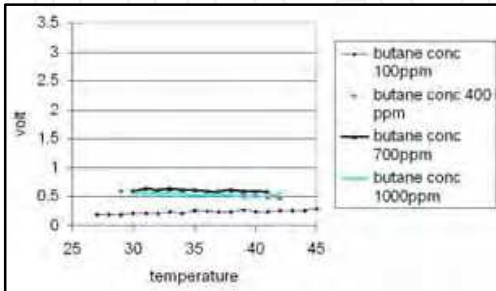


Fig. 25. Butane with TGS 2600 at  $R_L$

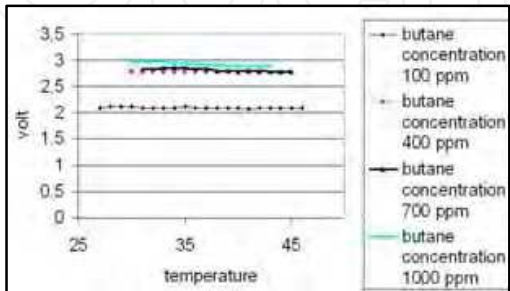


Fig. 26. Butane with TGS 2600 at  $R_L$  7

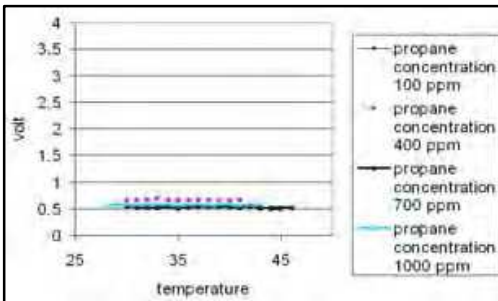


Fig. 27. Propane with TGS 2600 at  $R_L$

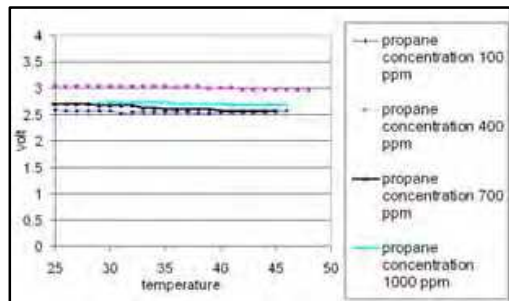


Fig. 28. Propane with TGS 2600 at  $R_L$  7

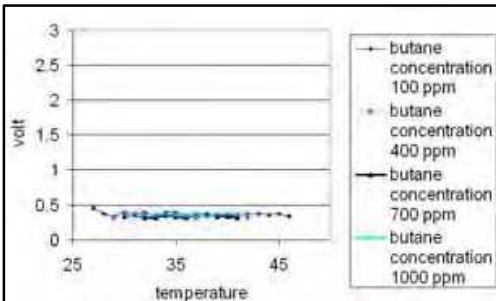


Fig. 29. Butane with TGS 4160 at  $R_L$

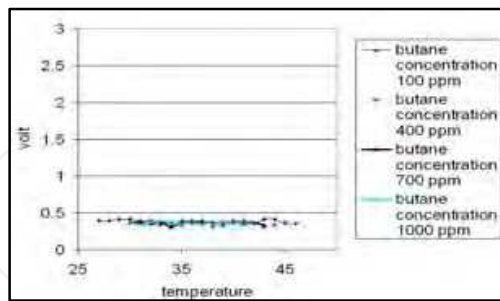


Fig. 30. Butane with TGS 4160 at  $R_L$  7

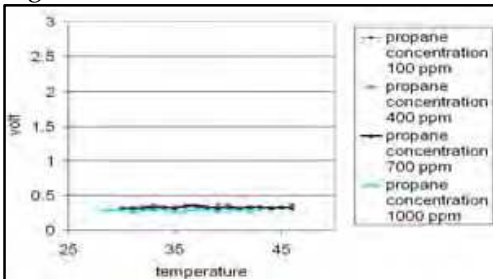


Fig. 31. Propane with TGS 4160 at  $R_L$  1  $k\Omega$

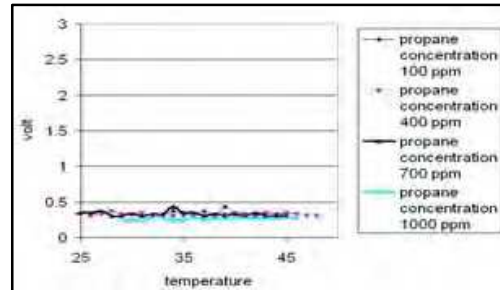


Fig. 32. Propane with TGS 4160 at  $R_L$  7  $k\Omega$



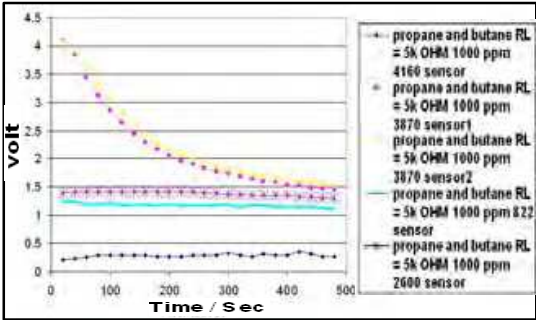


Fig. 33. Mixture of propane and butane at  $R_L$  1 k $\Omega$

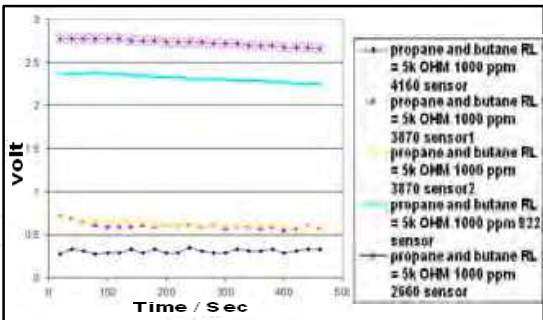


Fig. 34. Mixture of propane and butane at  $R_L$  7 k $\Omega$

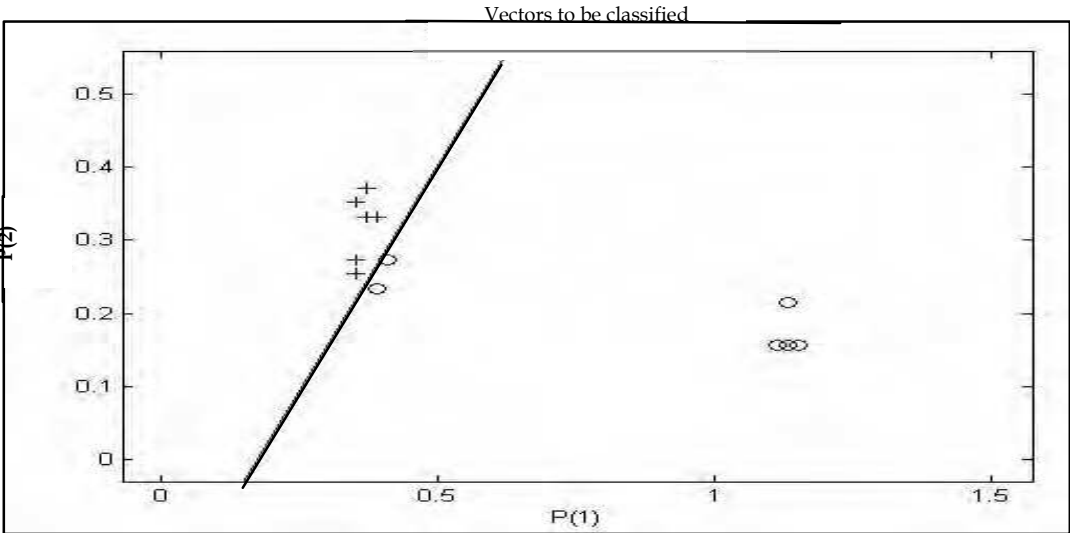


Fig. 35. Separation between propane and butane using NN(MLP) with TGS 822

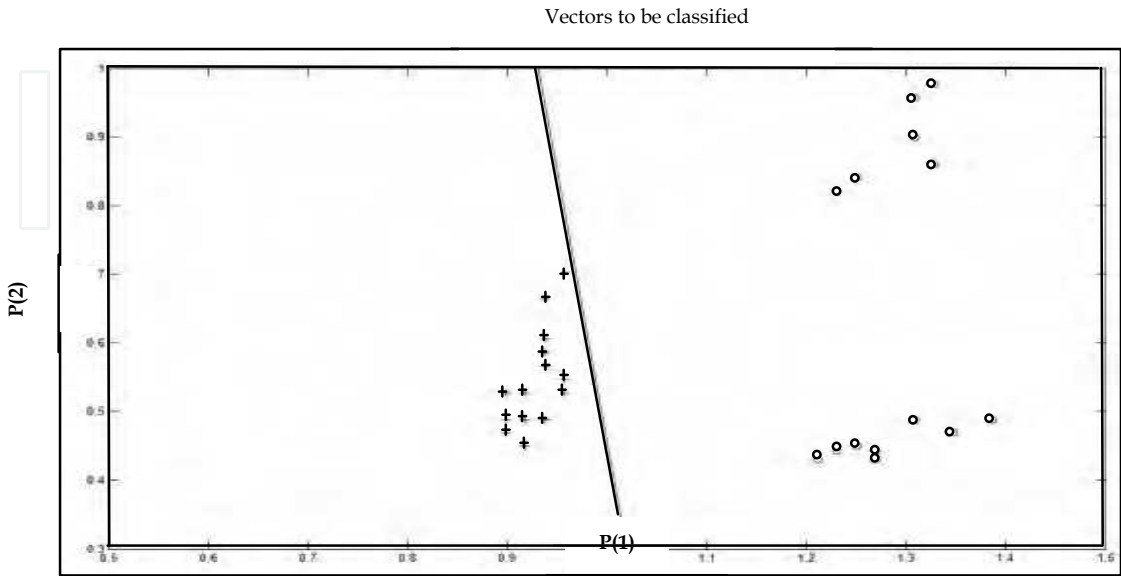


Fig. 36. Separation between propane and butane using NN (MLP) with TGS 3870



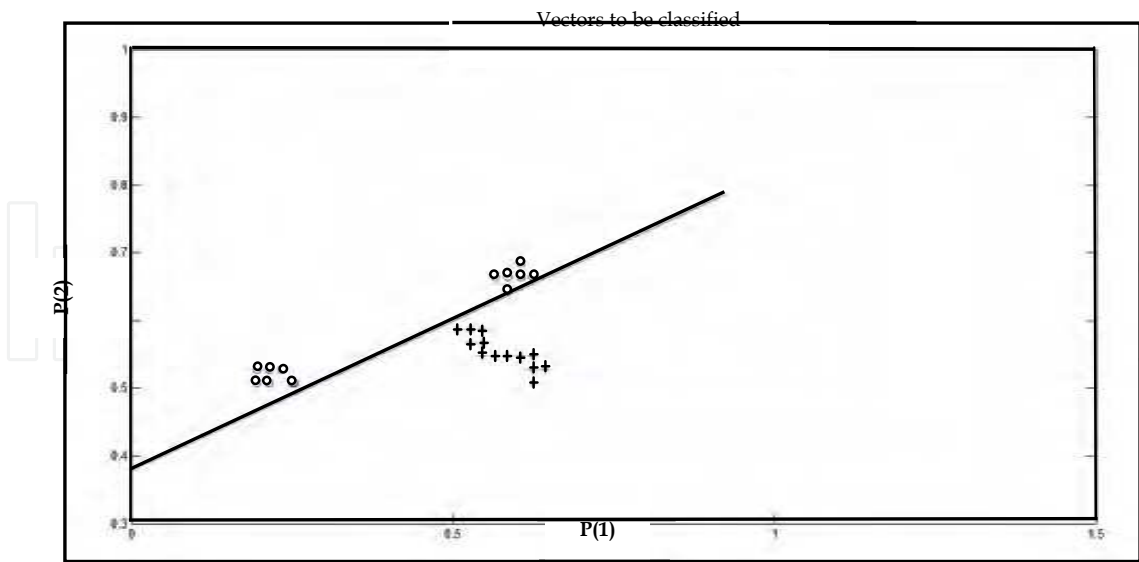


Fig. 37. Separation between propane and butane using NN (MLP) with TGS 2600

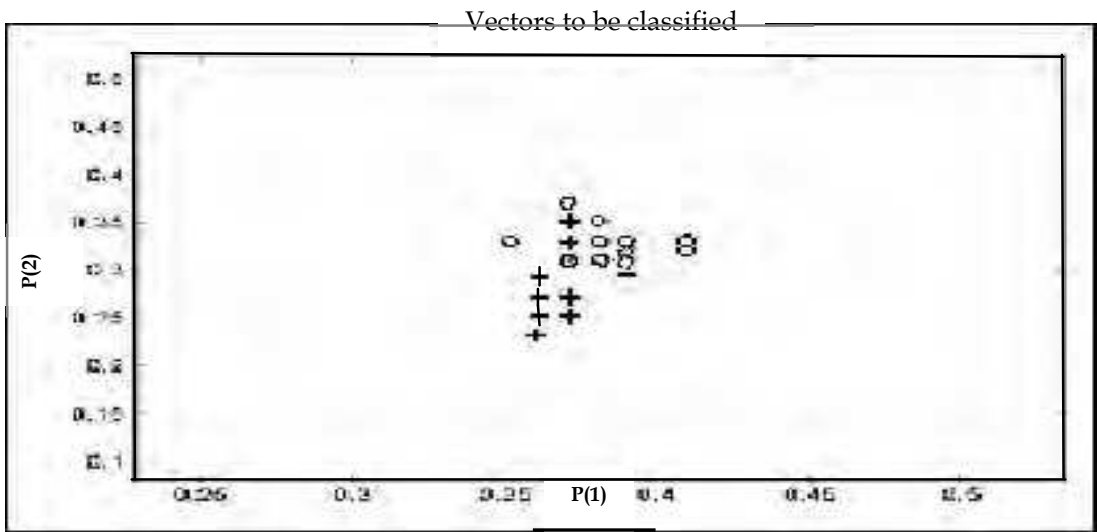


Fig. 38. Separation between propane and butane using NN (MLP) With TGS 4160

Sensors	No. of inputs	No. of output	Test	Epoch	% Error	Classificatio n	% Unflassificatio n
TGS 822	3 (100 sample)	1 (100 sample)	30 sample	1000	0.662%	60%	40%
TGS 3870	3 (100 sample)	1 (100 sample)	30 sample	1000	0.031%	97%	3%
TGS 2600	3 (100 sample)	1 (100 sample)	30 sample	1000	0.162%	96%	14%
TGS 4160	3 (100 sample)	1 (100 sample)	30 sample	1000	1.5%	40%	60%

Table. 5. The results of classification by using Neural Networks (MLP) for four different sensors.

## 6. On- Line Identification of Gases Using Artificial Intelligent Technique of Fuzzy Logic:

Fuzzy set theory and fuzzy logic theory are the preferred choices for the models. Fuzzy sets introduced were particularly designed to mathematically represent fuzziness and vagueness, and to provide the fundamental concept for handling the imprecision intrinsic to the problems of subjective evaluation and measurement. Fuzzy set is based on possibility instead of probability where as fuzzy logic is based on fuzzy set. Fuzzy logic is unlike classical logical systems in that it aims to modeling the imprecise modes of reasoning that plays an essential role in the remarkable human ability to make rational decisions in gases of uncertainty and imprecision. This ability depends, in turn, on the ability to infer an approximate answer to a question based on a store of knowledge that is inexact, incomplete, or not totally reliable. The whole approach is based on measurements taken from an experimental set up with certain typical commercial sensors. The outputs of sensors are monitored by a microcontroller, and then a proper intelligent processing. Fuzzy logic has been chosen because it gives better results and enhances discrimination techniques among sensed gases. Fuzzy logic systems encode human reasoning to make decisions and control dynamical systems. Fuzzy logic comprises fuzzy sets which are methods of representing nonstatistical uncertainty and approximate reasoning, including the operations used to make inferences. It is a tool for mapping the input features to the output, based on data in the form of "IF - Then" rules. An implementation of a fuzzy expert system depends on Mamdani type fuzzy controller as shown in fig. 39 (Tanaka, 1996); (Timothy, 1995); (Wesley, 1997). The objective of the controller is to discriminate different gases and to detect the concentration of each gas according to the input variables as shown in fig. 40. There are five steps to construct a Mamdani type fuzzy controller:

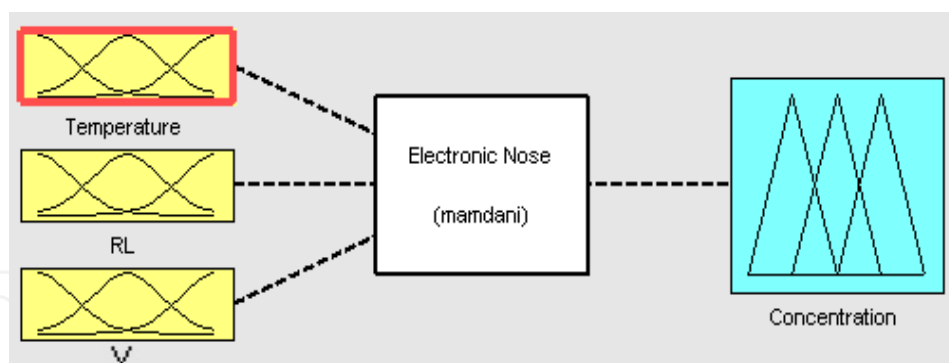


Fig. 39. Mamdani type fuzzy controller

Step 1: Identify and name the input linguistic variables, the output linguistic variables and their numerical ranges. There are three input variables which are temperature, output voltage of the microcontroller, and the variable resistance related to each sensor. The output variable is the concentration of each gas. There are five identified ranges for each variable (Morsi , 2007)

Temperature (°C)		Output volt of microcontroller (V)	
Linguistic Range		Linguistic Range	
Low	$20 < T < 30$	V. Low	$0.5 < V < 1.5$
Moderate	$25 < T < 35$	Low	$1 < V < 2$
Medium	$30 < T < 40$	Medium	$1.5 < V < 2.5$
High	$35 < T < 45$	High	$2 < V < 3$
V. High	$40 < T < 50$	V. High	$2.5 < V < 3.5$
Variable Resistance (KΩ)		The concentration of each gas in (ppm)	
Linguistic Range		Linguistic Range	
V. Low	$1 < R_L < 3$	V. Low	$100 < \text{concentration} < 400$
Low	$2 < R_L < 4$	Low	$250 < \text{concentration} < 550$
Medium	$3 < R_L < 5$	Medium	$400 < \text{concentration} < 700$
High	$4 < R_L < 6$	High	$550 < \text{concentration} < 850$
V. High	$5 < R_L < 7$	V. High	$700 < \text{concentration} < 1000$

Step 2: Define a set of fuzzy membership functions for each of the input and the output, variables. The low and high values are used to define a triangular membership function. The height of each function is one and the function bounds do not exceed the high and low ranges listed above for each range. The membership functions must cover the dynamic ranges related to the minimum and maximum values of inputs and outputs that represent the universe of discourse.

Step 3: Construct the rule base that will govern the controller’s operation. The rule base is represented as a matrix of input and output variables. At each matrix row different input variable ranges with one of the output variable range. All rules are activated and fired in parallel whether they are relevant or not and the duplicate ones are removed to conserve computing time. Each rule base is defined by ANDing together with the inputs to produce each individual output response. For example, If temperature is low AND, if voltage is low AND if,  $R_L$  is low THEN concentration is low.

Step 4: The control actions will be combined to form the excited interface. The most common rules combination method is the centroid defuzzification to get the crisp output value. This step is a repeated process, after all adjustments are made, which allows the fuzzy expert system to be able to discriminate and classify the data set patterns of the different gases.

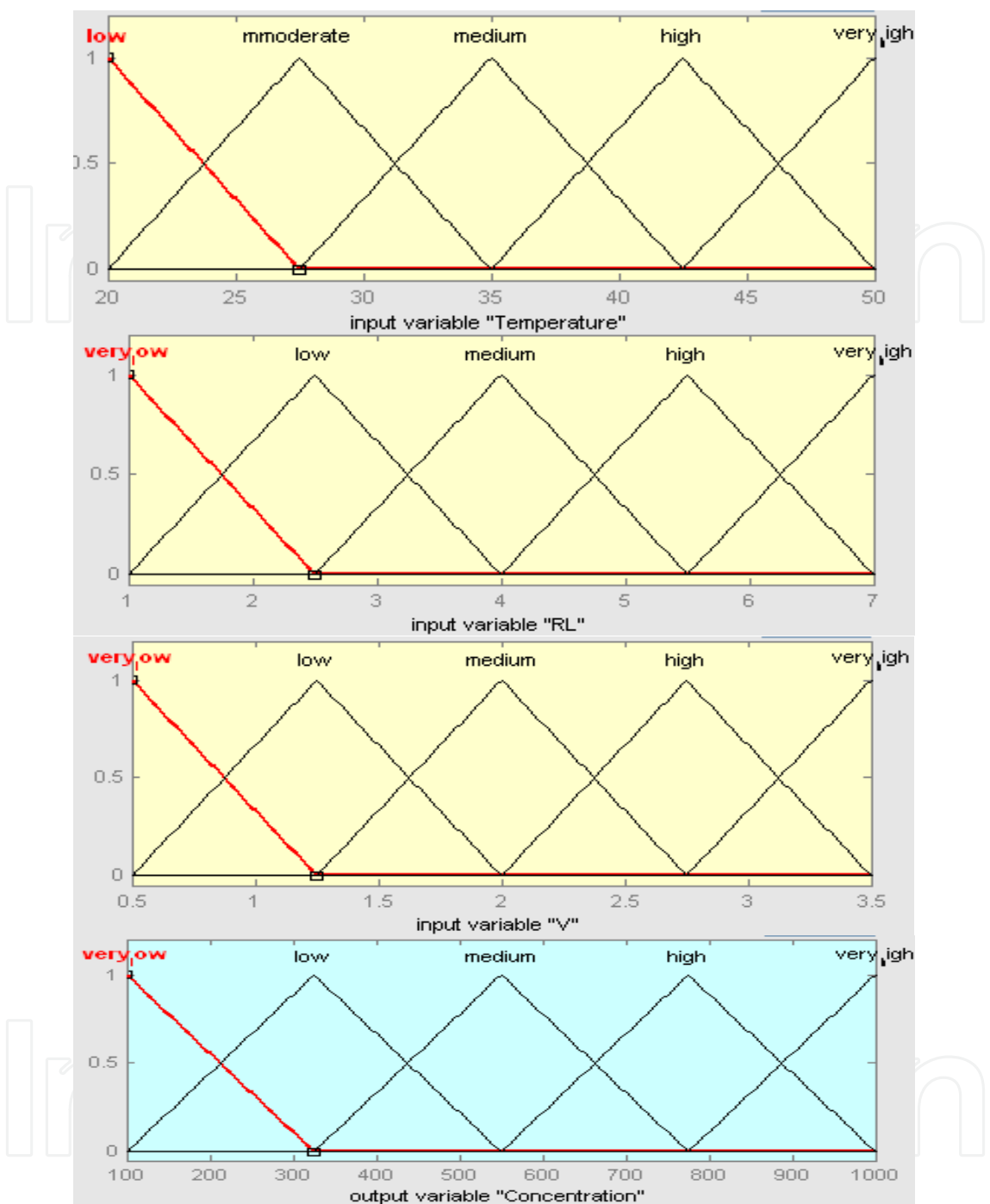
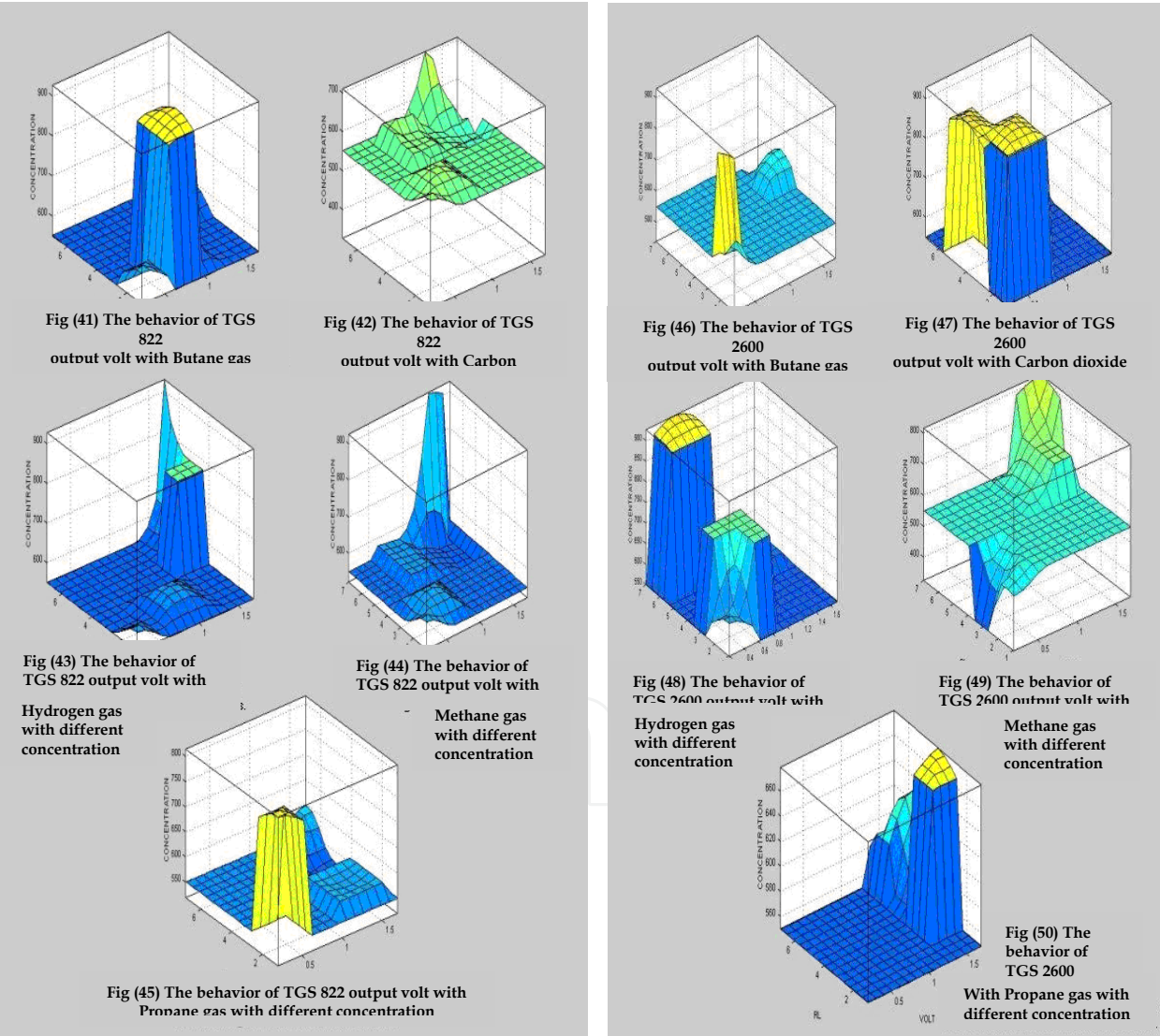
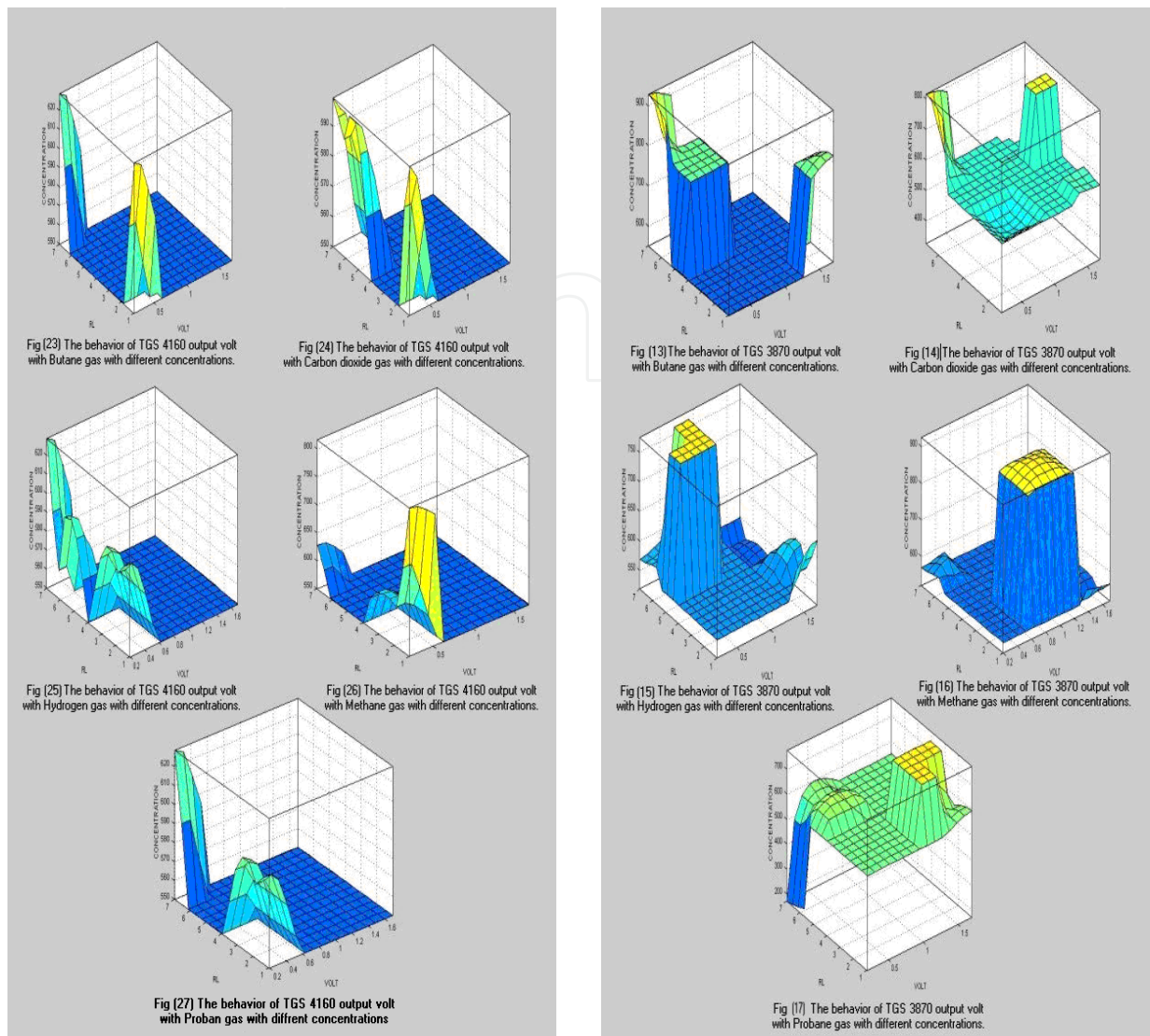


Fig. 40. Fuzzy membership functions with three input variables (Temperature, variable resistance, voltage of each sensor) and output variable (concentration).

Mamdani type fuzzy controller is used to construct the rules, which are extracted from the data driven from the microcontroller. It can be used to discriminate and classify the data set patterns for different gases according to the variation in different parameters, such as gas concentrations, variation in sensor's resistance and output voltage of microcontroller at different temperatures and to improve the sensor's selectivity for gas identification. Due to the abundant number of membership function figures, the results are limited to representing the fuzzy logic output surface for each sensor. Fuzzy logic gives on line prediction of the concentration depending on the behavior of each gas with different sensors which are extracted from the experiments. The feature of each gas is detected, based on the fuzzy system. The input and output surface of the fuzzy inference system is illustrated in figs 41-60 (Morsi, 2007).







7. Conclusion

The large scale of data is able to provide high-level information to make decisions about each gas achieved by using efficient and affordable sensor systems that show autonomous and intelligent capabilities. Measurements have been done using an electronic nose design, depending on commercially available gas sensors. An enormous data collected allows analyzing and characterizing of different gases. Several tests have been carried out by eliminating from the complete time series, a subset of data in a random way to evaluate the reliability of the developed model. The data set is characterized by several problems which can generate errors during processing and prediction phases inducing:

- Missing data, caused by the periodic setting or the stop function of instruments.
- Incorrect recording data occurred by errors in transmission, recording and non-setting of equipment.

Some interpolation and validation techniques to address and solve the above problems depend on building a mathematical model based on a suitable regression analysis and interpolation, which is able to describe the behaviour of daily average concentration. The aim of modeling for gases studies is to describe the peculiar characteristics of gases as alarm situations or risk events. Electronic nose provides, low cost, low maintenance small size, and in some cases low power consumption. The system can handle problems such as sensor drift, noise and non-linearity. It is used as a simple alarm level based on index data. This could be used as a stepping stone for the development of more complex systems, which are needed for more demanding applications.

## 8. Acknowledgement:

I would like to express my sincere gratefulness and gratitude to Prof. Dr. Moustafa Hussein Professor of Optical Communications and OSA member. Vice Dean for education and research affairs, College of Engineering and Technology in Arab Academy for Science, Technology and Maritime Transport, e-mail [mosaly@aast.edu](mailto:mosaly@aast.edu), for his tolerance in revising the chapter as well as his endless guidance and support.

## 9. References:

- Amigoni, F.; Brandolini, A.; Caglioti, V.; Lecce, V.; Guerriero, A.; Lazzaroni, M.; Lombardi, F.; Ottoboni, R.; Pasero, E.; Piuri, V.; Scotti, O. & Somenzi, D. (2006). Agencies for perception in environmental monitoring. *IEEE Transactions on Instrumentation and Measurement*, Vol. 55, No.4, (august 2006), pp. (1038 – 1050), DOI 10.1109/ TIM, 2006. 877747.
- Becker, I.; Muhlberger, S.; Bosch, C.; Braunmuhl, V., Muller, G.; Meckes, A. & Benecke, W. (2000). Gas mixture analysis using Micro – reactor systems. *IEEE Journal of micro electromechanical systems*, Vol.9, No.4, (december 2000), pp. (478 – 484), DOI S1057 – 7157 (00) 10867-4.
- Bourgeois, W.; Romain, A.; Nicolas, J. & Stuetz, R. (2003). The use of sensors arrays for environmental monitoring: interests and limitations. *J. Environmental, Monitoring*, Vol.5, (october 2003), pp (852 – 860), ISSN: 10. 1039 / b 307905h.
- Belhovari, S.; Bermak, A.; Wei, G. & Chan, P. (2004), Gas identification algorithms for microelectronic gas sensor, *Proceeding of instrumentation and Measurement Technology*, pp. 584 – 587, ISBN 0-7803 – 8248 Como, (may 2004), IMTC 2004, Italy.
- Belhovari, S.; Shi, M.; Bermark, A. & Chan, P. (2005). Fast and robust gas identification system using an integrated gas sensor technology and gaussian mixture models. *IEEE Sensors Journal*, Vol.5, No.6, (december – 2005), pp. (1433 – 1444), DOI 510.1109/ JSEN, 2005. 858926.
- Belhovari. S.; Shi, M.; Bermark, A. & Chan, P. (2006). Gas identification based on committee machine for micro electronic gas sensor. *IEEE Transactions on Instrumentation and measurement*, Vol. 55, No.5, (october 2006), pp (1786 – 1793), DOI S10.1109/TIM. 2006. 880956.
- Clifford, K.H.; Robinson, A.; David, R. & Mary, J. (2005) Overview of sensors and needs for environmental monitoring. *Sensors*, Vol. 5, No. 28, (february 2005), pp. (4-37), ISSN 1424 – 8220.

- Carullo, A. (2006). Metrological management of large – scale measuring systems. *IEEE Transactions on Instrumentation and Measurement*, Vol. 55, No.2, (april 2006), pp. (471-476), DOI 10.1109/ TIM. 2006. 870125.
- Dong Lee, D. & Sik Lee, D. (2001). Environmental gas sensor. *IEEE Sensors Journal*, Vol.1, No.3, (october 2001), pp. (214 – 217), ISSN 1530 – 437 x (01) 09470-2.
- Eberhart, R.; Simpson, P. & Dobbings, R. (1996). *Computational Intelligence PC Tools, APPROFESSIONAL*, ISBN 0-12-228630-8, USA>
- Fleming, W. (2001). Overview of automotive sensors. *IEEE Sensors Journal*, Vol. 1, No.4, (december 2001), pp. (296 – 308), ISSN S1530-437X (01) 11158-9.
- Getino, J.; Gutierrez, J.; Ares, L.; Robla, J.; Sayago, C.; Horrillo & Gap, J. (1995). Integrated sensor array for gas analysis in combustion atmosphere, *Proceeding on solid- state sensors and Actuators*, pp. 803 – 806, Stockholm, (june 1995), Transducers 95 Euro sensors 1x, Sweden.
- Guardado J.; Naredo, J.; Moreno, P. & Fuerte, C. (2001). A Comparative Study of neural network efficiency in power transformers diagnosis using dissolved gas analysis, *IEEE Transactions on Power Delivery*, Vol. 16, No.4, (october 2001), pp. 643-647, ISSN 0885 – 8977 (01) 08497-7.
- Ishida, H.; Nakayama, G., Nakamoto, T. & Morizumi, T. (2005). Controlling a gas/odor plume tracking robot based on transient responses of gas sensors. *IEEE Sensors Journal*, Vol.5, No. 3. (june 2005), pp. (537 – 545), DOI 10.1109 / ISEN, 2051 – 839597.
- Josphine, B. & Subramanian, V. (2008). Electronic noses sniff success. *IEEE Spectrum*, Vol.45, No.3, (march 2008), pp. (47 – 53), ISSN 0018 – 9235.
- Kolen, P. (1994). Self- calibration / compensation technique for microcontroller based sensors arrays. *IEEE Transactions on Instrumentation and measurement*, Vol. 43, No.4, (august 1994), pp. (620 – 623), ISSN 0018 – 9456 / 94.
- Luo, R.; Chen, C. & Luo, Y. (2002). Multisensor fusion and integration: approaches, applications and future research directions. *IEEE Sensors Journal*. Vol. 2, No.2, (april 2002), pp. 107-119. ISSN S 1530 – 437x (02) 03941 – 6.
- Marco, S.; Ortega, A.; Pardo, A. & Samitier, J. (1998). Gas identification with tin oxide sensor array and self organizing maps: adaptive correction of sensor drifts. *IEEE Transactions on Instrumentation and Measurement*, Vol. 47, No.1, (february 1998), pp. (316-321), ISSN 0018 – 9456..
- Morsi, I. (2007). A microcontroller based on multisensors data fusion and artificial intelligent technique for gas identification. *Proceeding of IEEE Industrial Electronics Society*, pp 2203 – 2208, ISBN 1-4244 – 0783 – 4107, Taipei, (november 2007), industrial electronics society, Taiwan.
- Morsi-a, I. (2008). Discrimination of some atmospheric gases using an integrated sensor array, surface response modeling algorithms and analysis of variance (ANOVA), *Proceeding of IEEE Sensors and Application Symposium (SAS)*, pp. 140 – 145, ISBN 978 – 1 – 4244 – 1963 – 0108, Atlanta, (february 2008), IEEE Sensors, USA.
- Morsi-b, I. (2008). Discrimination between butane and propane in a gas mixture using Semiconductor gas sensors and neural networks, *Proceeding of IEEE Sensors Application Symposium*, pp. 134-139, ISBN 978 – 1- 4244 – 1963 – 0108, Atlanta, (february 2008), IEEE Sensors, USA.
- Morsi – b, I. (2008). Electronic noses for monitoring environmental pollution and building regression model, *Proceeding of IEEE Industrial Electronics Society*, pp. 1730 – 1735.

- ISBN 978 - 1 - 4244 - 1766 - 7108 Orlando, (november 2008), IEEE industrial electronics society, Florida.
- <http://www.figarosensor.com> (on line).
- Smulko, J. (2006). The measurement setup for gas detection by resistance fluctuations of gas sensors, *Proceeding on Instrumentation and Measurement Technology*, pp. 2028 - 2031, ISBN 0-7803, 9360, 0106, Sorrento, (april 2006), IEEE instrumentation and measurement society, Italy.
- Timothy, J. (1995). *Fuzzy Logic with Engineering Applications*, McGraw- Hill INC, ISBN 0-07-053917-0, New York.
- Tanaka, K. (1996). *An Introduction to Fuzzy Logic for Practical Applications*, Springer, ISBN 0-387-94804-4, New York.
- Wesley, J. (1997). *Fuzzy and Neural Approaches in Engineering*, John Wiley & Sons INC, ISBN 0-471-19247-3, 1, USA.
- Wilson, D.; Hoyt, S.; Janata, H.; Booksh, K. & Obando, L. (2001). Chemical sensors for portable handheld field instruments. *IEEE Sensors Journal*, Vol.1, No.4 (december 2001), pp. (256-274), ISSN 1530 - 437X (01) 11120 - 6.
- Weigong, J.; Chen, Q., Reu, M.; Liu, N. & Daoust, C. (2006). Temperature feedback control for improving the stability of a semiconductor metal oxide (SMO) gas sensor, *IEEE Sensor Journal*, Vol. 6, No.1, (february 2006), pp. 139 - 145, ISSN 10.1109/ JSEN, 2005. 844353.
- Zylka, P. & Mazurek, B. (2002). Rapid dissolved gas analysis by means of electrochemical gas sensor, *Proceeding of 14<sup>th</sup> International conference on Dielectric Liquids*, pp. 325 - 328, ISBN 0-7803 - 7350 - 2102, Graz, (july 2002), ICDL 2002, Austria.



## **Data Storage**

Edited by Florin Balasa

ISBN 978-953-307-063-6

Hard cover, 226 pages

**Publisher** InTech

**Published online** 01, April, 2010

**Published in print edition** April, 2010

The book presents several advances in different research areas related to data storage, from the design of a hierarchical memory subsystem in embedded signal processing systems for data-intensive applications, through data representation in flash memories, data recording and retrieval in conventional optical data storage systems and the more recent holographic systems, to applications in medicine requiring massive image databases.

### **How to reference**

In order to correctly reference this scholarly work, feel free to copy and paste the following:

Iman Morsi (2010). Electronic Nose System and Artificial Intelligent Techniques for Gases Identification, Data Storage, Florin Balasa (Ed.), ISBN: 978-953-307-063-6, InTech, Available from:  
<http://www.intechopen.com/books/data-storage/electronic-nose-system-and-artificial-intelligent-techniques-for-gases-identification>



### **InTech Europe**

University Campus STeP Ri  
Slavka Krautzeka 83/A  
51000 Rijeka, Croatia  
Phone: +385 (51) 770 447  
Fax: +385 (51) 686 166  
[www.intechopen.com](http://www.intechopen.com)

### **InTech China**

Unit 405, Office Block, Hotel Equatorial Shanghai  
No.65, Yan An Road (West), Shanghai, 200040, China  
中国上海市延安西路65号上海国际贵都大饭店办公楼405单元  
Phone: +86-21-62489820  
Fax: +86-21-62489821



© 2010 The Author(s). Licensee IntechOpen. This chapter is distributed under the terms of the [Creative Commons Attribution-NonCommercial-ShareAlike-3.0 License](https://creativecommons.org/licenses/by-nc-sa/3.0/), which permits use, distribution and reproduction for non-commercial purposes, provided the original is properly cited and derivative works building on this content are distributed under the same license.

IntechOpen

IntechOpen